

Energy effectiveness of ocean-going cargo ship under various operating conditions

Sui, Congbiao; Stapersma, Douwe; Visser, Klaas; de Vos, Peter; Ding, Yu

DOI

[10.1016/j.oceaneng.2019.106473](https://doi.org/10.1016/j.oceaneng.2019.106473)

Publication date

2019

Document Version

Final published version

Published in

Ocean Engineering

Citation (APA)

Sui, C., Stapersma, D., Visser, K., de Vos, P., & Ding, Y. (2019). Energy effectiveness of ocean-going cargo ship under various operating conditions. *Ocean Engineering*, 190, Article 106473. <https://doi.org/10.1016/j.oceaneng.2019.106473>

Important note

To cite this publication, please use the final published version (if applicable). Please check the document version above.

Copyright

Other than for strictly personal use, it is not permitted to download, forward or distribute the text or part of it, without the consent of the author(s) and/or copyright holder(s), unless the work is under an open content license such as Creative Commons.

Takedown policy

Please contact us and provide details if you believe this document breaches copyrights. We will remove access to the work immediately and investigate your claim.



Energy effectiveness of ocean-going cargo ship under various operating conditions

Congbiao Sui^{a,b}, Douwe Stapersma^b, Klaas Visser^b, Peter de Vos^b, Yu Ding^{a,*}

^a College of Power and Energy Engineering, Harbin Engineering University, Harbin, 150001, China

^b Faculty of Mechanical, Maritime and Materials Engineering, Delft University of Technology, the Netherlands

ARTICLE INFO

Keywords:

Ship propulsion system
Electric power generating system
Energy conversion effectiveness
Fuel consumption
Energy management
Power-take-off

ABSTRACT

The increasing economic cost and environmental impact of maritime transportation necessitate the reduction of fossil fuel consumption of ocean-going cargo ships. Although fundamental ship propulsion system theory is well-known and is at a mature stage of development, there is still an enormous variety in the assessment methodology of (environmental) transport performance of ships. Furthermore, calibration of ship propulsion system model parameters with testbed, towing tank and full-scale measurement data is rare, as these measurements are both difficult and expensive. Finally, the effects of different power management strategies on the ultimate energy conversion effectiveness of typical cargo ships have rarely been investigated systematically. In this paper these three issues are discussed, addressed and solved for a representative benchmark chemical tanker. This ship was chosen to investigate the so-called energy conversion effectiveness under various propulsion control and electric power generation modes, as ample real ship data is available. The transport performance assessment of the ship's power plant is generalised for hybrid arrangements with either Power-Take-Off or Power-Take-In. The results show that an optimal combination of propulsion control, power management and voyage planning will further reduce the global fuel consumption and CO₂ emissions produced by the shipping industry.

1. Introduction

Almost 70 years ago, in (Gabielli and Von Karman, 1950), Gabielli and Von Karman asked the question, 'What Price Speed?'. In this classic paper, the economic cost for faster travel by means of various transport modes was investigated from an efficiency perspective. Today, due to increasing economic and environmental pressure, high maximum speed is no longer the highest priority in design and operation for transportation vehicles, especially for maritime transport (Lindstad and Eskeland, 2015). Thus, priority has shifted to the question 'What Price Transportation?' rather than 'What Price Speed?' (Eyring et al., 2010; Shi, 2013).

Fuel consumption significantly influences the economic cost of transportation and directly results in the emission of carbon dioxide (CO₂), which is a major greenhouse gas (Lindstad et al., 2013). Consequently, the overall fuel consumption includes not only the economic cost, but also the environmental impact (Psarafitis and Kontovas, 2010). The shipping industry, being the main carrier of world trade carrying over 80% by volume and more than 70% of its value (UNCTAD, 2017), consumes much more fuel than other transport modes, in spite of the fact

that shipping is the most energy-efficient mode of cargo transport (Øyvind et al., 2003).

The increasing worldwide concerns regarding the environmental impact of maritime transportation thus necessitate proper evaluation and reduction of fossil fuel consumption of commercial ships, particularly cargo ships. In order to facilitate the ship performance evaluation, during both the ship preliminary design stage and operation stage (Coraddu et al., 2014), a consistent and comprehensive theoretical framework is indispensable. During ship operation, propulsion control and power management significantly influence the fuel consumption performance of ships (Armstrong and Banks, 2015; Geertsma et al., 2017a), so quantitative and systematic investigations in this regard is needed when trying to improve the transport performance of ships.

1.1. Existing frameworks and terminology

It is difficult to properly assess the ship transport performance due to the large amounts of influencing variables (Coraddu et al., 2015). Indicators and criteria for transport performance of ships need to be identified when evaluating ship performance (Misra, 2016). Thus, research has been performed to quantify the transport performance of

* Corresponding author. address: No. 145, Nantong Street, 150001, Harbin, China.

E-mail address: dingyu@hrbeu.edu.cn (Y. Ding).

Nomenclature*Roman symbols*

AC	alternating current
AG	auxiliary generator
C_E	specific ship resistance (-)
C_E^*	normalised specific ship resistance (-)
C_{fuel}	correcting factors of fuel consumption (-)
CPP	controllable pitch propeller
ECI	energy conversion index
EPI	effective power index
FI	fuel index (g/(ton-mile))
GB	gearbox
HFO	heavy fuel oil
I	current of electricity (A)
J	propeller advance coefficient (-)
J^*	ratio of propeller advance coefficient (-)
K_Q	propeller torque coefficient (-)
K_Q^*	ratio of propeller torque coefficient (-)
K_T	propeller thrust coefficient (-)
K_T^*	ratio of propeller thrust coefficient (-)
LHV	lower heating value (kJ/kg)
MCR	maximum continuous rating
M_D	delivered torque to propeller (Nm)
m_D	dead weight tonnage of the ship (t)
MDF	marine diesel fuel
M^*	normalised engine torque (-)
M_{eng}	engine torque (Nm)
m_f	injected fuel mass per cycle (kg)
m_f^*	normalised injected fuel mass per cycle (-)
N^*	normalised engine speed (-)
n^*	ratio of propeller speed (-)
n_{eng}	engine speed (r/s)
$P_{AG,e}$	electric power of auxiliary generator (W)
$P_{B,aux}$	power of auxiliary engines (W)
$P_{B,main}$	power of main engines (W)
$P_{B,E}$	engine power for electrical loads (W)
$P_{B,P}$	engine power for propulsion (W)
$P_{B,PTO}$	engine power for PTO (W)
P_D	delivered power to propeller (W)
P_D^*	ratio of delivered power (-)
P_E	ship effective power (W)
P_E^*	ratio of the ship effective power (-)

$P_{E,max}$	maximum ship effective power (W)
P_{Elec}	electrical power of onboard grid (W)
P_M	mobility power of ship (W)
P_{max}	maximum combustion pressure (MPa)
$P_{SG,e}$	electrical power of shaft generator (W)
$P_{SG,m}$	mechanical power of shaft generator (W)
PTO	power take off
R	towing resistance of ship (N)
R_{max}	maximum ship resistance (N)
sfc	specific fuel consumption (g/kWh)
SG	shaft generator
SM	sea margin (-)
t	thrust deduction fraction (-)
TI	transport index
U	voltage of electricity (V)
V	ship speed (m/s)
v_s	ship speed (m/s)
v_s^*	normalised ship speed (-)
V_{max}	maximum ship velocity (m/s)
w	wake fraction (-)
W_D	deadweight of ship (N)
W_G	gross weight of ship (N)

Greek Symbols

ε_{EC}	energy conversion effectiveness (-)
ε_{EP}	ship effective power effectiveness (-)
ε_{hub}	hub distribution factor (-)
ε_T	transport effectiveness (-)
η_0^*	ratio of propeller open water efficiency (-)
η_D	propulsive efficiency (-)
η_D^*	ratio of propulsive efficiency (-)
η_{eng}	engine efficiency (-)
η_H	ship hull efficiency (-)
η_R^*	ratio of relative rotation efficiency (-)
η_{TRM}	transmission efficiency (-)
ρ	density of water (kg/m ³)
Φ_{FE}	energy flow of fuel to engines (J/s)
$\Phi_{FE,aux}$	energy flow of fuel to auxiliary engines (J/s)
$\Phi_{FE,main}$	energy flow of fuel to main engine (J/s)
$\Phi_{Fuel,main}$	fuel mass flow into main engine (g/h)
$\Phi_{Fuel,aux}$	fuel mass flow into auxiliary engines (g/h)
ϕ	phase angle between voltage and current (deg)
ω_p	angular speed of propeller (rad/s)

ships and marine vehicles (Papanikolaou, 2014; Stapersma, 2017). The EEDI (Energy Efficiency Design Index) proposed by IMO (International Maritime Organisation) (MEPC, 2014), which for merchant ships is the obligatory indicator defining the ship energy efficiency, is in principle the ratio of penalty to benefit of the energy conversion of ships (Stapersma, 2016). As such, the EEDI has a close relationship to the energy conversion effectiveness that will be introduced in this paper. The main difference is however that the energy conversion effectiveness is defined for different ship speeds and for representative environmental conditions, while the EEDI is not. In (Papanikolaou, 2005), the *transport efficiency* is defined as the ratio of the total installed power to the vessel's deadweight or payload times the ship service speed. In (Akagi, 1991), the *reciprocal transportation efficiency* is defined as a function of the ship displacement, maximum ship speed and total installed power. In (Akagi and Morishita, 2001), the *specific power* is analysed as a function of the ship payload, maximum ship speed and total installed power. In (Kennell, 1998), a *transport factor* is defined as a function of the ship's displacement, the design speed and the total installed power. The

above-mentioned indicators of ship transport performance are essentially the same or similar while they may be termed differently by different researchers.

1.2. Influence of ship operations

Reducing the fuel consumption is an effective solution to decrease the transportation cost and the emission of greenhouse gases (Stapersma, 2010; Bialystocki and Konovessis, 2016). Although the design of the ship propulsion system initially influences the fuel consumption behaviour of the ship (Altosole et al., 2007), ship operation plays a crucial role in the fuel consumption reduction as well (Roskilly et al., 2015; Andersson et al., 2016). A practical and widely adopted practice to reduce fuel consumption of cargo ships is reducing ship speed, both during design (decrease design speed) and operationally (slow steaming). (Psarafitis and Kontovas, 2013; Lee et al., 2015). However, using only one single design point to calculate EEDI rather than the actual operation on the basis of ship missions during its lifetime, IMO strives to

reduce installed power and thus design ship speed to achieve a smaller EEDI, raising serious concerns regarding the safety of ships in adverse conditions (Papanikolaou et al., 2016; Bitner-Gregerse et al., 2016). Instead, designing the ship with a higher design speed and reducing actual operational speed during missions could be more effective and, more importantly, safer (Yasukawa et al., 2017).

Ship propulsion control and energy management also influence the fuel consumption performance of ships significantly (Kanellos et al., 2014; Geertsma et al., 2017a, 2017b). In (Geertsma et al., 2017b), in a case study of a patrol vessel, Geertsma et al. find that propulsion control strategy can save up to 30% of fuel, while also reducing thermal engine loading and acceleration time. Further in (Geertsma et al., 2018), Geertsma et al. propose an adaptive pitch control strategy to optimise the fuel consumption, ship manoeuvrability, engine thermal loading and propeller cavitation noise. In (Buhag et al., 2009), an assessment of the energy-saving potential using known technology and practices has shown that a proper energy management can reduce CO₂ emissions (CO₂/ton·mile) by 1–10% as a result of reduction of fuel consumption. In (Figari and Guedes Soares, 2009), Figari, et al. propose a ‘dynamic set point’ propulsion control scheme with respect to the ‘static combinator’ control scheme for the best use of the ship propulsion system in terms of power, fuel consumption and exhaust emissions for a ferry.

1.3. Requirement of a flexible simulation tool

Simulation models can be categorized into two main groups: first principle and empirical models (Del Re et al., 2010). First principle models provide the ability to gain physical insight in the investigated systems and not just the superficial and direct results and therefore have always been the first choice of researchers (Guzzella and Onder, 2009; Del Re et al., 2010). First principle models have to be limited however, both in scope and depth, to balance the usefulness and effectiveness with required calculation time of the chosen models (Bossel, 1994; Refsgaard and Henriksen, 2004). In order to get to effective high-performance models, one of the common ways is combining the first principle and empirical approaches, from different aspects or at different levels, resulting in hybrid models (Asprion et al., 2013). In (Figari and Campora, 2003), a ship propulsion system model, which includes amongst others a complex two-zone crank angle diesel engine model based on Wiebe shaped combustion, but on the other hand a simple one-dimensional lookup table for the ship resistance model and simple two-dimensional lookup tables for the propeller model, is developed and used to analyse the components and system responses at off-design and transient conditions. For a better balance in (Schulten, 2005; Grimmelius et al., 2007; Sui et al., 2017; Geertsma et al., 2017b), ship propulsion system models containing different mean value first principle (MVFP) models of a diesel engine are developed for the investigation of ship performance. In (Vrijdag, 2009), in order to investigate the control of propeller cavitation in operational conditions, a complex propeller model and propulsion control model can be found in the ship propulsion system model while the diesel engine is modelled as a set of lookup tables. Thus, the complexity and focus of models depend on the goals pursued by researchers using the model. Sometimes it is accepted to have large differences in the level-of-detail of component models, but as a general rule-of-thumb the authors consider it better to strive for more balanced system models with approximately equivalent level-of-detail for all component models.

1.4. Existing problems and knowledge gap

The existing terminology defining the ship transport performance is considered to be inconsistent and confusing. The current terminology mixes up the concepts of ‘energy effectiveness’, ‘energy efficiency’ and ‘energy factor’ when defining the ship transport performance. Moreover, most of the indicators only take the power chain of ‘shaft to wheel’ (from installed power to ship mobility power) rather than ‘tank to wheel’ (from fuel energy flow to ship mobility power) into consideration neglecting

power generation, which can make significant differences to the overall transport performance of ships. When the engines are considered, most of the research of ship transport performance only focus on the input and output ends of the power chain of the energy conversion and fail to clarify the individual contributions of each part of the power chain to the overall performance. In addition, in most research, indicators of ship transport performance, including IMO’s EEDI, are only investigated at one single ship speed, often the design ship speed, rather than at various operational ship speeds and only in calm water conditions, which rarely is the case according to (Faltinsen, 1980).

The influence of propulsion control strategy on the fuel consumption performance have been researched for ships whose operating conditions change frequently, such as navy frigates, patrol vessels and Ro-Ro Pax ferries etc. However, quantitative and systematic investigations of the influence on the fuel consumption of ocean-going cargo ships, which consume much more fuel than any other ship type, by propulsion control as well as the adoption of a shaft generator (power-take-off, PTO) are scarce. This gap in maritime research is addressed in this paper.

1.5. Outline and goals

Thus, the main goals of this paper are:

1. To introduce a transport performance index called the energy conversion effectiveness. This performance indicator can be calculated for different ship speeds and representative environmental conditions and encompasses all energy conversions on board of ships (section 3).
2. Calibration of (the parameters of) a theoretic ship propulsion system model with extensive tank and on-board measurement data taken on board of a typical chemical tanker (i.e. full-scale measurements). The model is “balanced”, i.e. approximately equal level-of-detail of component models (section 4).
3. Investigation into the effects of different ship propulsion control and electric power generation modes on the energy conversion effectiveness and other performance variables in realistic sailing conditions (section 5).

Section 6 contains the conclusions, discusses limitations and uncertainties of the current study and provides recommendations for future work. But first, in chapter 2, a benchmark chemical tanker providing all the opportunities to systematically investigate the fuel consumption performance of ocean-going cargo ships, is introduced.

2. Benchmark ship and propulsion + electric power system

2.1. A representative benchmark ship: chemical tanker

A 13000 DWT chemical tanker (shown in Fig. 1), for which ample real ship measurement data (both towing tank and full-scale) are available, has been chosen as a benchmark for this study because it represents a “normal” type of ship that takes its share in the daily business of transportation of goods. The layout of the power plant, i.e. propulsion and electric power system, of the benchmark chemical tanker is shown in Fig. 2. The benchmark chemical tanker has a propulsion system, where a controllable pitch propeller (CPP) driven by a two-stroke main engine is installed. The propulsion system with CPP allows to investigate ship performance when operating in different propulsion control modes, i.e. Constant Revolution Mode, Constant Pitch mode and Combinator mode. The electric power generation system of the chemical tanker consists of a shaft generator that is powered by the main engine through a PTO gearbox and auxiliary generators driven by auxiliary diesel engines. The chemical tanker having a power generating system with PTO and auxiliary generators provides the opportunity to investigate the influence on the ship performance of different electric power generation modes, i.e. Aux mode and PTO mode. Both the propulsion control modes and electric power generation modes will be



Fig. 1. 13000 DWT chemical tanker (Courtesy of Ningbo Xinle Shipbuilding Group Co., Ltd).

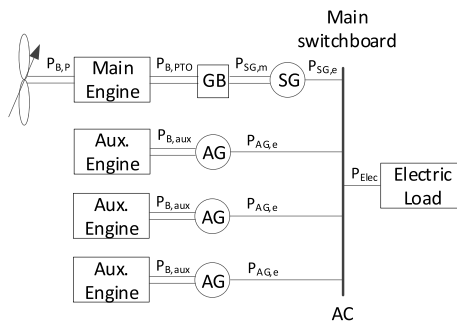


Fig. 2. Layout of the chemical tanker power plant (i.e. propulsion system and electric power generation + distribution system).

elaborated in section 5.2.

2.2. General information of the chemical tanker + power plant

Some general ship and power plant information of the chemical tanker is presented in Table 1 and Table 2.

3. Energy conversion effectiveness and fuel index

3.1. Energy conversion effectiveness

When evaluating the transport performance of ships that transport goods from one port to another the ultimate ship mission must be taken into account (Stapersma, 2017), i.e. the mobility power to move a certain useful weight with a certain speed should be added to the end of the power chain of the ship propulsion, as illustrated by Fig. 3. The main power is provided by the main engine for ship propulsion which overcomes ship resistance at a certain ship speed indicated by the ship effective power (Harvald, 1983; Molland et al., 2011). The auxiliary power is provided by the auxiliary engines, or by the main engine in PTO (power-take-off) mode, to support the ship auxiliary systems, the crew and the cargo, etc., mainly indicated by the electric power for on-board loads. The key connection between the main power and auxiliary power line in case of PTO is the mechanical “splitting” hub working together with an electrical “merging” hub, refer to Fig. 3.

In (Gabielli and Von Karman, 1950), in order to evaluate the transportation performance of ships, Gabielli and Von Karman defined the effective power index EPI (equal to the resistance/weight ratio)¹ as:

¹ The resistance/weight ratio which was originally termed as the coefficient of the specific resistance symbolized as ε by Gabielli and Von Karman was actually an index (cost/benefit) and hence will be called an effective power index EPI in this paper.

$$EPI = \frac{P_{E,max}}{W_G \cdot V_{max}} = \frac{R_{max}}{W_G} \quad (1)$$

where, $P_{E,max}$ is the maximum ship effective power, [W]; R_{max} is the maximum ship resistance, [N]; W_G is the ship gross weight, [N] and V_{max} is the maximum ship velocity, [m/s].

However, the effective power index EPI defined by equation (1) to evaluate the ship transportation performance has a number of drawbacks. Firstly, the maximum ship speed and the corresponding maximum ship effective power are used in the definition, which is not representative. Secondly, in the original paper, Gabielli and Von Karman themselves had already argued that a certain useful load which the ship transports rather than the gross weight of the ship should be used when evaluating the economic performance of transportation of the ship. They failed to do this finally due to lack of exact information. Last but not least, the definition by equation (1) only takes the hull resistance into account, i.e. excluding the ship propulsion and power generation. This, nowadays, cannot be neglected when analysing the energy conversion performance of the whole ship.

To solve the first and the second problem, in this paper the definition of the effective power index EPI has been improved to equation (2). The maximum ship speed and the corresponding maximum ship effective power have been replaced with the operational ones during real ship sailing. The ship gross weight has been replaced by ship dead weight, which following IMO is considered the “useful” weight.

$$EPI = \frac{P_E}{W_D \cdot V} = \frac{R}{W_D} \quad (2)$$

where, P_E is the ship effective power, [W]; R is the ship resistance, [N]; V is the ship speed, [m/s] and W_D is the dead weight of the ship, [N].

Extending the concept of the effective power index introduced by (Gabielli and Von Karman, 1950), the transport effectiveness ε_T of ships is defined by equation (3):

$$\varepsilon_T = \frac{W_D \cdot V}{P_{B,P}} \quad (3)$$

where, $P_{B,P}$ is the engine power required for ship propulsion, [W].

Note that effectiveness essentially is a benefit/cost ratio. In the definition of the transport effectiveness ε_T by equation (3), the ship propulsion and transmission system are included. In order to also include the engine power generation and take both the main engine and auxiliary engines into account, the energy conversion effectiveness ε_{EC} is according to (Stapersma, 2017) defined by equation (4):

$$\varepsilon_{EC} = \frac{W_D \cdot V}{\Phi_{FE,main} + \Phi_{FE,aux}} \quad (4)$$

where, $\Phi_{FE,main}$ is the fuel energy flow into the main engine, [J/s]; $\Phi_{FE,aux}$ is the fuel energy flow into the auxiliary engines, [J/s].

Decomposing the energy conversion effectiveness ε_{EC} unveils the different elements of the power chain of the ship. Equation (5) shows that the energy conversion effectiveness ε_{EC} is the product of familiar component efficiencies, a power distribution factor ε_{hub} and a ship effective power effectiveness ε_{EP} :

$$\varepsilon_{EC} = \underbrace{\frac{P_{B,main} + P_{B,aux}}{\Phi_{FE,main} + \Phi_{FE,aux}}}_{\eta_{eng}} \cdot \underbrace{\frac{P_{B,P}}{P_{B,main} + P_{B,aux}}}_{\varepsilon_{hub}} \cdot \underbrace{\frac{P_D}{P_{B,P}}}_{\eta_{TRM}} \cdot \underbrace{\frac{P_E}{P_D}}_{\eta_D} \cdot \underbrace{\frac{W_D \cdot V}{P_E}}_{\varepsilon_{EP}} = \eta_{eng} \cdot \varepsilon_{hub} \cdot \eta_{TRM} \cdot \eta_D \cdot \varepsilon_{EP} \cdot \varepsilon_T \quad (5)$$

Where, $P_{B,main}$ is the power of the main engine, [W]; $P_{B,aux}$ is the power of the auxiliary engines, [W]; P_D is the delivered power to the propeller, [W].

The hub distribution factor ε_{hub} defined in equation (5) includes the engine power required for ship propulsion, since only that power in the end is “useful” and benefits the mobility power, and the engine power

Table 1
General information of the chemical tanker and the propulsion system.

Particulars of the Chemical Tanker	Main Engine			Propeller	
Length Between Perp. [m]	113.80	Type	MAN 6S35ME (2-stroke)	Manufacturer	MAN ALPHA
Breadth Molded [m]	22.00	Rated Power [kW]	4170	Type	CPP
Depth Molded [m]	11.40	Rated Speed [rpm]	167	Nominal Revolution Rate [rpm]	167
Design Draught [m]	8.50	Stroke [m]	1.55	Number of Blades	4
Design Displacement [m ³]	16988	Bore [m]	0.35	Diameter [m]	4.30
Design Speed [kn]	13.30	P _{max} at MCR [MPa]	18.5		

Table 2
General information of the electric power generation system.

Auxiliary Gensets	Shaft Generator		
Number of Sets	3	Number of set(s)	1
Engine output [kW]	750	PTO gearbox output [kW]	1100
Generator output [kW]	712	Generator output [kW]	1045
Engine Speed [rpm]	900	PTO input speed [rpm]	167
Generator Speed [rpm]	900	Generator Speed [rpm]	1800
Generator Frequency [Hz]	60	Generator Frequency [Hz]	60

produced by both main and auxiliary engines. Note that the introduction of the hub distribution factor also makes it possible to define the combined engine efficiency that takes all power generation on board into account and consequently all fuel consumption.

If it is assumed that the power of both main engine and auxiliary engines is provided only for ship propulsion and on-board electrical loads, looking at the total engine power in the denominator from a different perspective, i.e. to where it will be consumed rather than from where it is generated, the definition of hub distribution factor ϵ_{hub} in equation (5) can then be written as equation (6):

$$\epsilon_{hub} = \frac{P_{B,P}}{P_{B,P} + P_{B,E}} \quad (6)$$

where, $P_{B,E}$ is engine power required by electrical loads, [W] and in our case is either equal to $P_{B,PTO}$ (in case of PTO) or $P_{B,aux}$ (in case of auxiliary engines running), see Fig. 3. In case of PTO and auxiliary engines running in parallel, $P_{B,E}$ is the sum of $P_{B,PTO}$ and $P_{B,aux}$, but this case will not be investigated in this paper. Note that, for the same electric power required by electric loads, the corresponding engine power $P_{B,E}$ in case of PTO is slightly larger than that in case of auxiliary engines running due to the power losses in the PTO gearbox. When the auxiliary engines would be (partly) used for power-take-in (PTI) the expression will be

different and more complicated but this paper will not look into PTI.

The hub distribution factor ϵ_{hub} is determined by the loads according to which the power distribution or energy management decisions are made, put even more poignantly, the hub distribution factor ϵ_{hub} defined in equations (5) and (6) actually is an “energy management factor” rather than an “energy usage efficiency”.

3.2. Fuel index

Fuel consumption of the ship at each operating point are quantified by the fuel index (FI , g/(ton·mile)), which is defined by equation (7).

$$FI = \frac{\Phi_{Fuel,main} + \Phi_{Fuel,aux}}{m_D \cdot V} \quad (7)$$

where, $\Phi_{Fuel,main}$ is the fuel mass flow into the main engine, [g/h]; $\Phi_{Fuel,aux}$ is the fuel mass flow into the auxiliary engines, [g/h]; m_D is the dead weight tonnage of the ship, [t]; and V is the ship speed, [kn].

Note that an index essentially is the inverse of effectiveness, i.e. a cost/benefit ratio.

4. Explanation and final calibration of propulsion system model

4.1. Propulsion system model description and philosophy

The models of the main components of the ship propulsion system as presented earlier in Fig. 2, although having a first principle structure with normalised in- and output variables, basically are empirical models fitted with a finite number of parameters (rather than look-up tables in which the measured test data are stored directly). The component models are given in Appendix A and were calibrated first to available test data (component level) as presented in Appendix B. The component models were integrated into the overall ship propulsion and electric generating system model of the chemical tanker using first principle

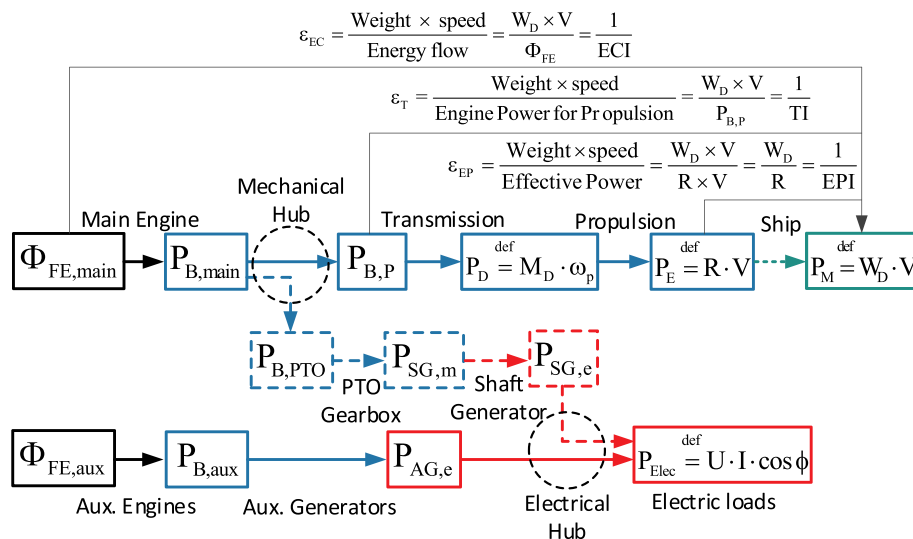


Fig. 3. Energy conversion in the propulsion system and electric power generating system.

balances as shown in Fig. 4. In this case the propulsion system model could also be validated by sea trial test data (system level) of the real ship and the actual matching of engine, propeller and ship be established as shown in the following sections. This should make the subsequent results of the analysis very realistic as the model is based on hard full-scale data.

4.2. Correction of towing tank measurement data and model calibration using sea trial measurements

First the results of resistance test of ship model and results of open water test of propeller model were directly used in building the simulation models of the ship resistance and the propeller open water characteristics, the details of which are given in Appendix B. However, there were discrepancies between the original model test prediction results of the delivered power and propeller speed at various ship speeds and the results of the real ship sea trial test. During the sea trial test, the shaft power was measured, from which the delivered power can be deduced assuming a transmission efficiency for the shaftline. Further propeller speed at various ship speeds was measured. Based on this, the original model test results of the chemical tanker have been corrected according to the sea trial test data. The correction procedure will be briefly introduced in the following.

To compare the sea trial test results and the model prediction results and get the multiplicative correction factors for the model test results,

ratios of relevant parameters of the sea trial test to those of the model prediction results are formed as shown in equation (8).

$$X^* = \frac{X_{trial}}{X_{prediction}} \tag{8}$$

The ratios according to equation (8) can be derived from relevant variables with the added advantage that constant quantities (such as sea water density and propeller diameter) are removed from the considerations. Note that ship speed is dropping out since all comparisons are made for the same ship speed. For all other quantities it is assumed that there can be a difference between the sea trial test and model prediction results. The correction factors for delivered power P_D^* and propeller speed n^* were determined using the sea trial results. These are the basis and final criterion for correction of the other parameters. Actually, there are many different solutions to correct the model prediction results by choosing different combinations of parameters having uncertainties that could be corrected.

It is assumed that the ship effective power and propeller characteristic rather than the relative rotation efficiency, thrust deduction fraction and wake fraction are the most uncertain factors. Therefore, the relative rotation efficiency, thrust deduction fraction and wake fraction are left out of the correction, in other words, they remain the same as the original model test data. Further assume that the propulsive efficiency which is the ratio of the ship effective power to the delivered power remains the same as the original model test prediction resulting in the

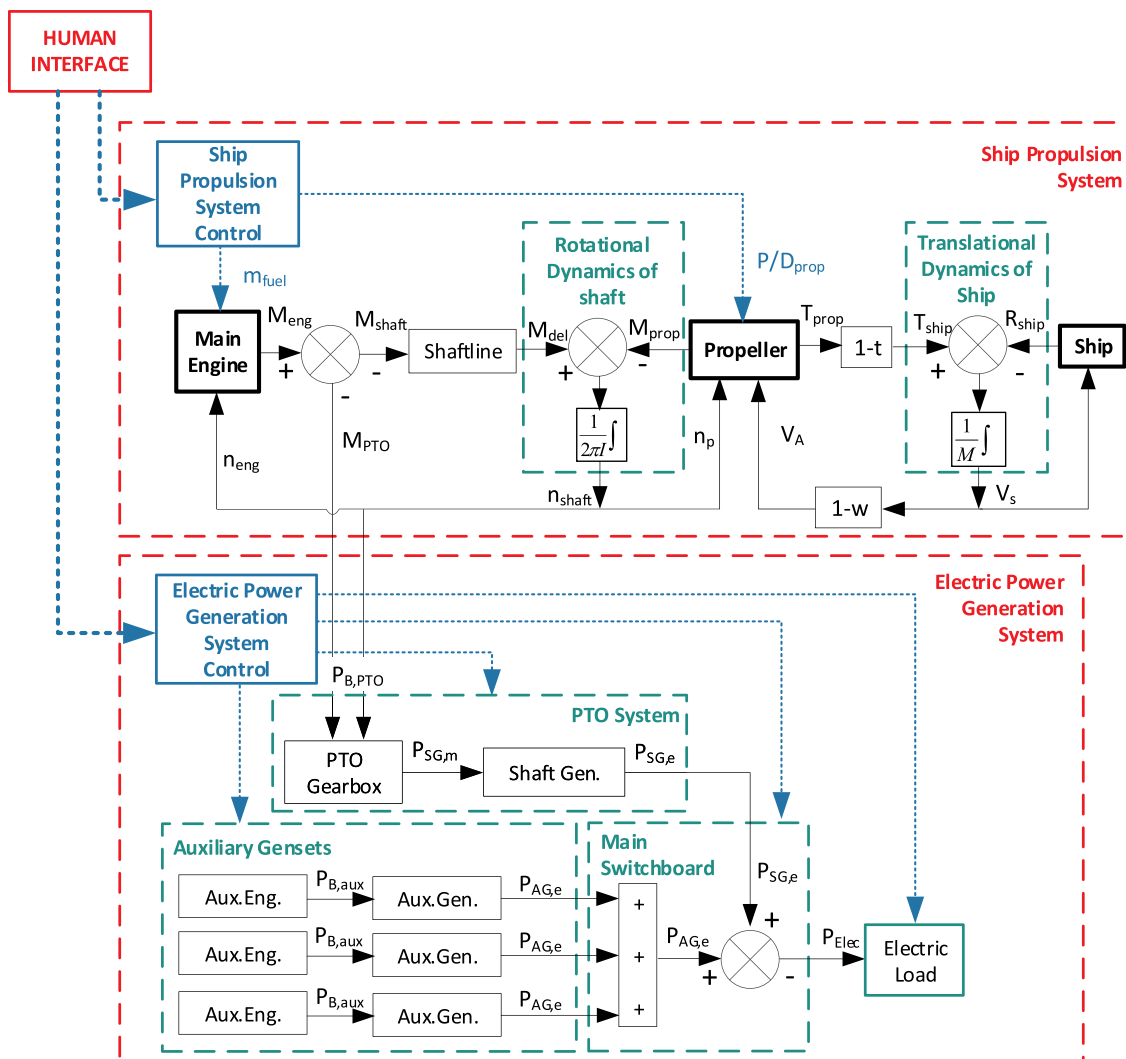


Fig. 4. Structure scheme of integrated ship propulsion and electric generating systems model of the chemical tanker.

same correction factor for the ship effective power and delivered power as shown in equation (9).

$$P_E^* = P_D^* \quad (9)$$

Then the correction factors for the propeller open water characteristics can be derived from those for the delivered power, propeller speed and ship effective power as shown in equations (10)–(12).

$$K_Q^* = \frac{P_D^* \cdot \eta_R^*}{(n^*)^3} = \frac{P_D^* \cdot 1}{(n^*)^3} = \frac{P_D^*}{(n^*)^3} \quad (10)$$

$$J^* = \frac{(1-w)^*}{n^*} = \frac{1}{n^*} \quad (11)$$

$$K_T^* = \frac{P_E^*}{(n^*)^2 \cdot (1-t)^*} = \frac{P_E^*}{(n^*)^2 \cdot 1} = \frac{P_E^*}{(n^*)^2} \quad (12)$$

$$\eta_0^* = \frac{K_T^* \cdot J^*}{K_Q^*} = \frac{P_E^*}{(n^*)^2} \cdot \frac{1}{n^*} \cdot \frac{(n^*)^3}{P_D^*} = \frac{P_E^*}{P_D^*} = 1 \quad (13)$$

Where P_D^* is the ratio of delivered power, n^* is the ratio of propeller speed, K_Q^* is the ratio of propeller torque coefficient, η_R^* is the ratio of relative rotation efficiency, $(1-w)^*$ is the ratio of wake fraction defect, J^* is the ratio of propeller advance coefficient, P_E^* is the ratio of the ship effective power, $(1-t)^*$ is the ratio of thrust deduction fraction defect, K_T^* is the ratio of propeller thrust coefficient, η_D^* is the ratio of propulsive efficiency and η_0^* is the ratio of propeller open water efficiency.

As argued, the result presented in equation (13) implies that the propeller open water efficiency at the same ship speed will remain the same as the original model test data as a result of the chosen solution for the corrections. Finally, the values of the correction factors deduced with the procedure above are presented in Table 3.

The model test results corrected using the above-mentioned method have been applied in developing and calibrating the models of propeller and ship resistance as introduced in Appendix B.

After the components models of the ship propulsion system have been built, the static matching of the ship propulsion system is analysed, matching to be understood as the relation between engine envelope and propeller/ship characteristic as fully explained in (Klein Woud and Stapersma, 2002). The matching results have been validated by the real ship sea trial test, shown in Fig. 5. The original matching based on the original model test data is “heavier” compared with the sea trial test results. Note that, due to the fact that there is only one overall set of correction factors as given in equation (10)–(12) and presented in Table 3, the measured points of the sea trial are still not all exactly on the model data but at least the model now correlates in a mean sense to the measured data. Note that the ship draught during sea trial test was the same as the ship design draught. In this paper, the service margin or sea

margin (SM) is assumed to be zero (SM = 0) during the sea trial test, despite of the fact that the wind force was actually Beaufort 3–4 and the sea state was Douglas 2–3 rather than a very calm sea, however the correction on resistance would be even larger if the sea margin during sea trials was noticeably larger than one.

5. Application of calibrated propulsion system model on the benchmark ship: simulation results for realistic operational conditions

5.1. Selecting a sea margin for typical sailing conditions

According to (Klein Woud and Stapersma, 2002), the sea margin (SM) in realistic sailing condition, which accounts for the added ship resistance due to the fouling of hull and propeller, displacement, sea state and water depth, as shown in equation (14), is selected relative to the sea margin of 0% in sea trial condition (calm water condition).

$$SM = f(\text{fouling}, \text{displacement}, \text{sea state}, \text{water depth}) = f_1(\text{fouling}) \cdot f_2(\text{displacement}) \cdot f_3(\text{sea state}) \cdot f_4(\text{water depth}) - 1 \quad (14)$$

Based on 1.5 years period and 3% increase of resistance per year due to fouling, the effect of hull and propeller fouling is:

$$f_1(\text{fouling}) = (1 + 0.03)^{1.5} = 1.045 \quad (15)$$

The ship resistance addition relative to that in trial condition due to sea state during realistic sailing conditions, taking wind, waves and currents in to account, is set to be 10%, so the effect of sea state is:

$$f_3(\text{sea state}) = 1.10 \quad (16)$$

Clearly this is a drastic simplification of actual sea state effects, but for the current design study it is deemed sufficient.

The draught of the ship during the sea trial test is the design draught, and it is assumed that the ship also sails at the design draught in real sailing condition. So, the effect of the displacement variations on ship resistance are neglected, see equation (17). Furthermore, it is assumed that the ship sails in deep water, as during the sea trials. So, the effect of shallow water on ship resistance is also neglected, see equation (18).

$$f_2(\text{displacement}) = 1 \quad (17)$$

$$f_4(\text{water depth}) = 1 \quad (18)$$

The total sea margin according to equation (14) will then be:

$$SM = 1.045 \times 1 \times 1.1 \times 1 - 1 = 0.15 \quad (19)$$

Table 3
Correction factors of ship model test data.

(a) Required correction factors for propeller speed, delivered power and ship effective power as concluded from sea trials				
Correction factors	n^*	$P_D^* = P_E^*$		
Value	0.9824	0.8580		
(b) Applied correction factors for specific resistance, wake factor, thrust deduction factor and relative rotative efficiency (chosen)				
Correction factors	C_E^*	$(1-w)^*$	$(1-t)^*$	η_R^*
Value	0.8580	1	1	1
(c) Applied correction factors for propeller characteristics (derived)				
Correction factors	J^*	K_T^*	K_Q^*	η_0^*
Value	1.0179	0.8890	0.9049	1

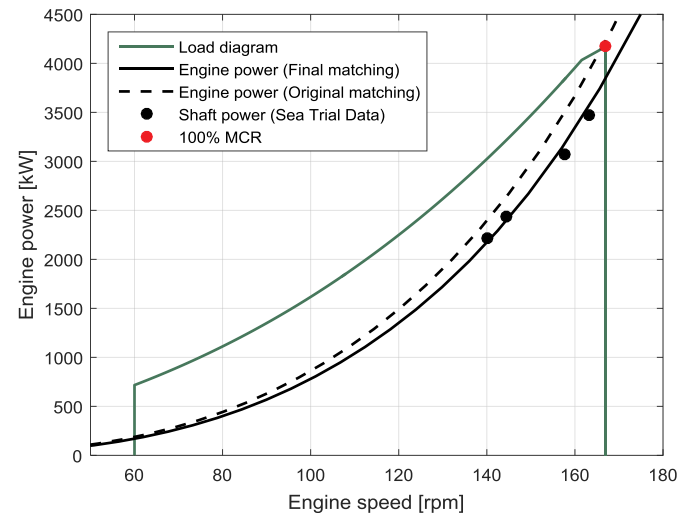


Fig. 5. Ship propulsion system static matching and validation.

Therefore, the sea margin (SM) in realistic sailing condition relative to sea trial condition is set to be 15%.

5.2. Different ship propulsion control and electric power generation modes

In this paper, different propulsion control modes as well as different electric power generation modes are taken into consideration to conduct a systematic ship propulsion behaviour investigation.

5.2.1. Ship propulsion control modes

A controllable pitch propeller, driven by the main engine is installed in the propulsion system of the chemical tanker. Theoretically, the chemical tanker propulsion system can work in three different control modes, namely Constant Revolution Mode, Constant Pitch mode and Combinator mode as presented in Table 4.

The propeller revolution and propeller pitch are predefined in combinator curves and controlled simultaneously by single lever command (SLC) for these three different propulsion control modes. In each combinator curve, for a given SLC, there will be a certain propeller revolution and propeller pitch. In constant revolution mode, the ship speed will be controlled by changing the propeller pitch and keeping the propeller revolution constant. In the constant pitch mode, the ship speed will be controlled by changing the propeller revolution and keeping the propeller pitch constant until the propeller revolution reaches the minimum revolution limit. In the combinator mode, the ship speed will be controlled by changing the propeller revolution (limited by the minimum and maximum revolutions) and pitch simultaneously, see Fig. 6 (a).

The mechanical power, which is either provided by the main engine to the shaft generator through the PTO gearbox in PTO mode or is provided by the auxiliary engine directly to the auxiliary generator in Aux mode, is 350 kW and assumed to be constant. Setting the sea margin as 15%, the operational results in terms of main engine speed and power under the Combinator control mode and the two electric power generation modes are shown in Fig. 6 (b).

When the electric power is generated in PTO mode, the main engine needs to provide extra power to the shaft generator in addition to the power required by the propulsion system. If the main engine is operating in the high engine speed region, in practice ship speed should be reduced somewhat or, for the sake of the engine operation safety, the electric power generation mode should be switched from PTO mode to Aux mode or the propeller pitch should be reduced slightly to keep the engine power inside the engine operating envelope.

5.2.2. Electric power generation modes

The electric power generation system of the chemical tanker consists of three auxiliary generators driven by three auxiliary engines and one shaft generator driven by the main engine through a PTO gearbox. The electric power required by the on-board electric loads can be provided either by the shaft generator (PTO mode) or by the auxiliary generators (Aux mode), or even by both the shaft generator and auxiliary generators working in parallel (Combined mode) when a large amount of electric power is needed in some special cases. The latter mode will however not be investigated in this paper. Table 5 presents the electric power generation modes investigated in this paper.

Table 4
Investigated propulsion control modes.

Constant Revolution Mode	CONSTANT revolution & CHANGING pitch (Generator Law)
Constant Pitch Mode	CONSTANT pitch & CHANGING revolution until minimum revolution is reached (Propeller Law)
Combinator Mode	CHANGING pitch & CHANGING revolution (limited by minimum and maximum revolution)

5.3. Correction for difference between diesel fuel type used in the engine test bed and real ship operations

The specific fuel consumption of the main engine is calculated by the diesel engine model introduced in the appendix. The specific fuel consumption of the auxiliary engine at 50% MCR is 230 g/(kWh) at ISO value for fuel LHV, and consequently the specific fuel consumption of the auxiliary engine, whose power at MCR is 750 kW, is assumed to be 230 g/(kWh) at ISO when it provides mechanical power of 350 kW to the auxiliary generator at Aux mode.

In reality, the diesel fuel type in ship operation is heavy fuel oil (HFO) for the main engine and marine diesel fuel (MDF) for the auxiliary engines. However, the fuel consumption test results measured on the engine test bed, which have been corrected at ISO, are used in developing and calibration of the main engine model. Therefore, the fuel consumption during real ship operation has been corrected according to equation (20) using the correcting factors shown in Table 6. Note that the underlying idea of equation (20) is that engine efficiency remains the same when changing fuel type.

$$\Phi_x = C_x \cdot \Phi_{x,ISO} \quad (20)$$

Where, Φ_x is the fuel consumption of HFO and MDF, [kg/s]; $\Phi_{x,ISO}$ is the fuel consumption of fuel at ISO, [kg/s]; C_x is the correcting factors of fuel consumption for different fuel types represented in Table 6.

5.4. Results and evaluation

The ship performance under different propulsion control modes as well as different power generation modes at nominal sea margin (SM = 15%) has been investigated and the results are presented in Figs. 7–14.

5.4.1. Fuel consumption and fuel index

The combined engine power and fuel flow at different propulsion control modes and power generation modes are shown in Fig. 7(a) and (b) respectively. According to Fig. 7 (a), the combined engine power in PTO mode is slightly higher than that of Aux mode because of the power losses in the PTO gearbox through which the power from the main engine is transmitted to the shaft generator while the power from auxiliary engine is directly transmitted to the auxiliary generator. According to Fig. 7 (b), the combined fuel flow at Aux mode is higher than that at PTO mode especially at low ship speeds due to the higher specific fuel consumption at Aux mode as shown in Fig. 8(a). For the same ship speeds, the constant revolution mode requires the highest engine power and fuel flow followed by the combinator mode and the constant pitch mode requires the lowest. This in fact is mainly caused by the lower propeller efficiency when the pitch is reduced in case of constant revolution and combinator mode compared with the constant pitch mode, as will be elaborated in the next section.

The combined specific fuel consumption (*sfc*) under constant revolution control mode is better than the constant pitch mode and the combinator mode especially at low ship speed as shown in Fig. 8 (a) while the results of fuel index (*FI*) under the three different propulsion control modes are contrary, as shown in Fig. 8 (b). The reason is that the main engine almost operates in the same region of specific fuel consumption under the three different control modes at high ship speeds while it runs in quite different regions at low ship speeds and for the 2-stroke engines in the benchmark ship the constant revolution mode runs through a better region of *sfc* compared with the other two modes (note that for 4-stroke engines constant revolution normally has a worse *sfc* compared to constant pitch propeller curve). The fuel index is determined by the fuel consumption flow at a certain ship speed when the ship dead weight remains the same. The constant revolution control mode has a higher fuel consumption flow compared with the other two modes especially at low ship speeds as already shown in Fig. 7(b).

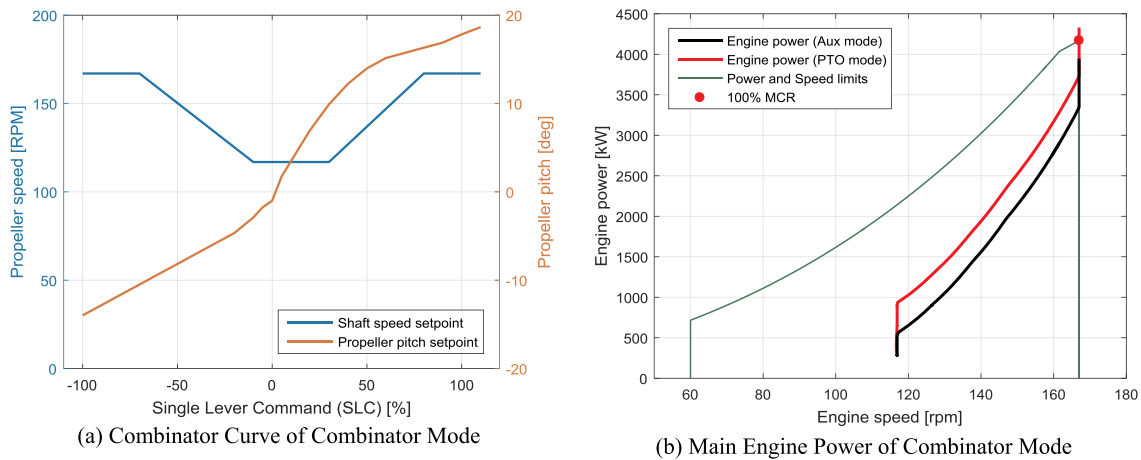


Fig. 6. Combinator curve as an example of one of the propulsion control modes.

Table 5

Investigated electric power generation modes.

PTO mode	Shaft generator ON & auxiliary generator OFF
Aux mode	Shaft generator OFF & auxiliary generator ON

Table 6

Correcting factors of fuel consumption.

Fuel Type	HFO	MDF
LHV [kJ/kg]	41500	42000
C_x [-]	1.0289	1.0167

Furthermore, the lowest fuel index under different propulsion control modes occurs at different ship speeds. It shows the fact that the fuel consumption can be reduced by slow steaming of the ship although the specific fuel consumption of the engines will increase with the reduction of the ship speed. Note that engine specific fuel consumption sfc is a combined value for main and auxiliary engines (if applicable) as implied by equation (5).

When looking at the electric power generation modes, the combined specific fuel consumption is higher at Aux mode than that at PTO mode especially at low ship speeds as shown in Fig. 8 (a). The reason is that, at low ship speeds, the engine power required for propulsion is low and the engine power for electric loads is relatively higher than at high ship speeds. Consequently, the auxiliary engine with higher specific fuel consumption contributes relatively more engine power at low ship

speeds resulting in higher combined specific fuel consumption at Aux mode. The difference between operating the shaft generator or auxiliary gensets also has some influence on the combined fuel index and the PTO mode has a lower fuel index in all the three propulsion control modes as shown in Fig. 8 (b).

The first lesson is that specific fuel consumption of the engine gives misleading trends and should not be used when considering the overall energy conversion in the ship. Instead the fuel index should be used since it contains information of the propeller efficiency and auxiliary power conversion as well and therefore is a real system performance indicator unlike sfc .

5.4.2. Energy effectiveness and efficiencies

The energy conversion effectiveness ϵ_{EC} shown in Fig. 10 is actually the inverse of the fuel index and thus the energy conversion effectiveness ϵ_{EC} has the inverse trend as that of the fuel index FI . The highest values of the energy conversion effectiveness correspond to the lowest values of the fuel index. In fact, the energy conversion effectiveness ϵ_{EC} is determined by the combined engine efficiency η_{eng} shown in Fig. 9, the hub distribution factor ϵ_{hub} shown in Fig. 11, the transmission efficiency η_{TRM} shown in Fig. 12, the propulsive efficiency η_D shown in Fig. 13 and the ship effective power effectiveness ϵ_{EP} which is actually the ratio of ship dead weight to ship resistance W_D/R shown in Fig. 14.

The combined engine efficiency η_{eng} shown in Fig. 9 is actually the inverse of the combined engine specific fuel consumption sfc shown in Fig. 8 (a). The hub distribution factor ϵ_{hub} , shown in Fig. 11, is determined by the propulsion load provided that the electrical load is kept

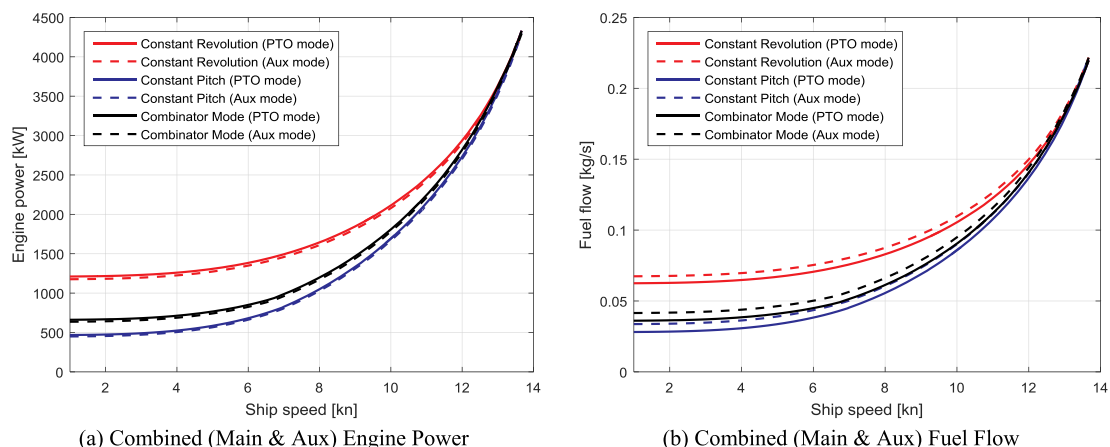


Fig. 7. Engine power and fuel flow (SM = 15%).

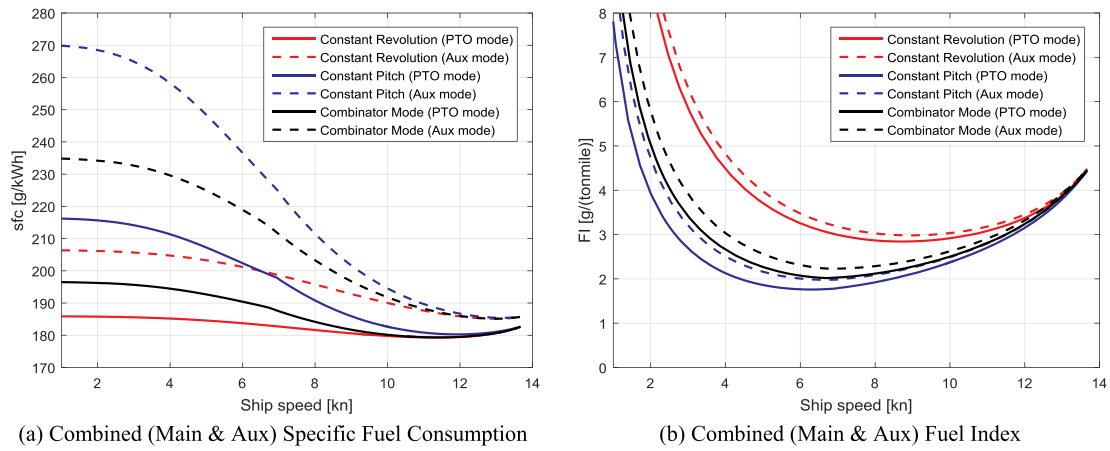


Fig. 8. Fuel consumption (SM = 15%).

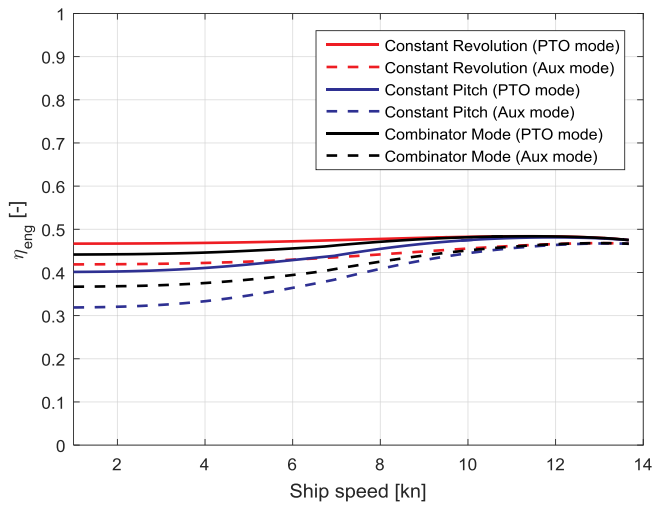


Fig. 9. Combined (main & Aux) engine efficiency.

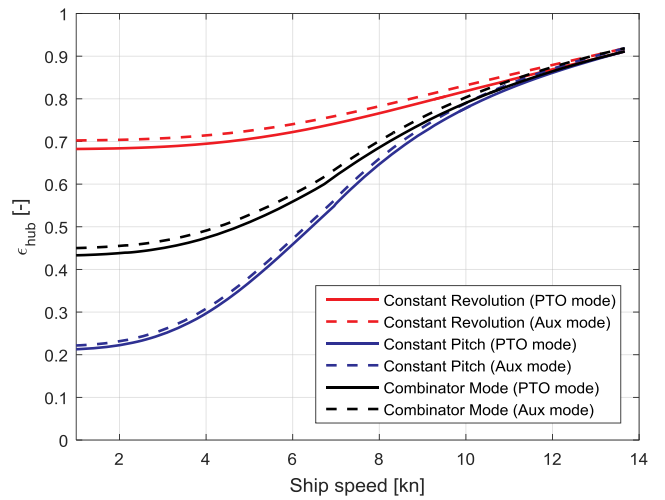


Fig. 11. Hub distribution factor.

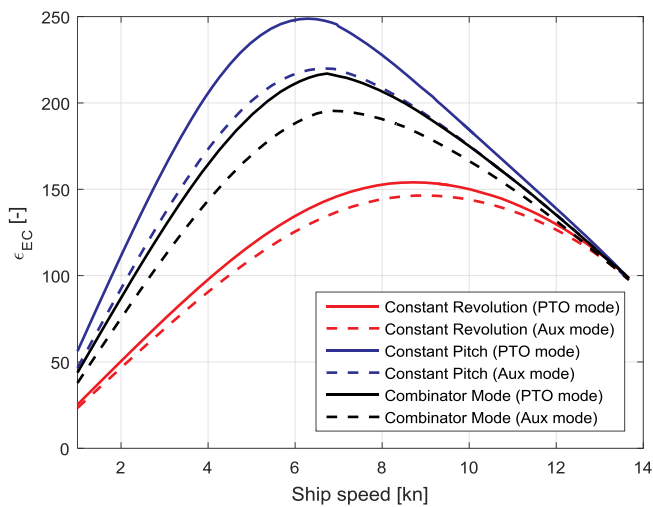


Fig. 10. Energy conversion effectiveness.

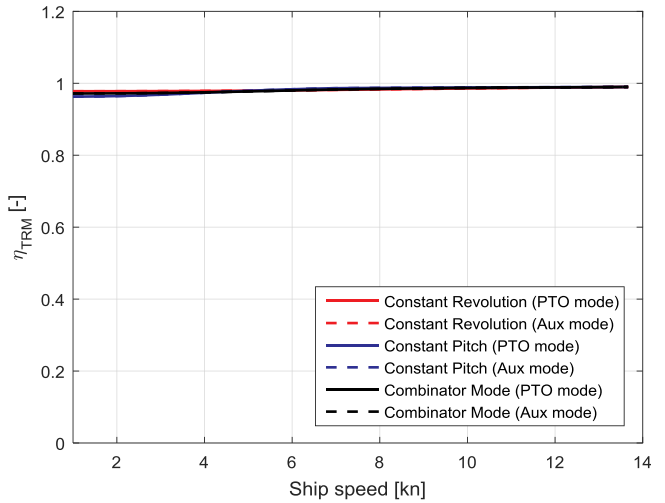


Fig. 12. Transmission efficiency.

constant, or rather, the hub distribution factor ϵ_{hub} will increase if the power required for ship propulsion increases. Both increasing the ship speed and changing propulsion control modes from constant pitch mode to constant revolution mode will increase the power required for

propulsion and consequently influence the hub distribution factor. In the latter case, it can be explained by the propulsive efficiency η_D of different control modes shown in Fig. 13. At certain ship speeds, in particular at low ship speeds, constant revolution mode with smaller propeller pitch

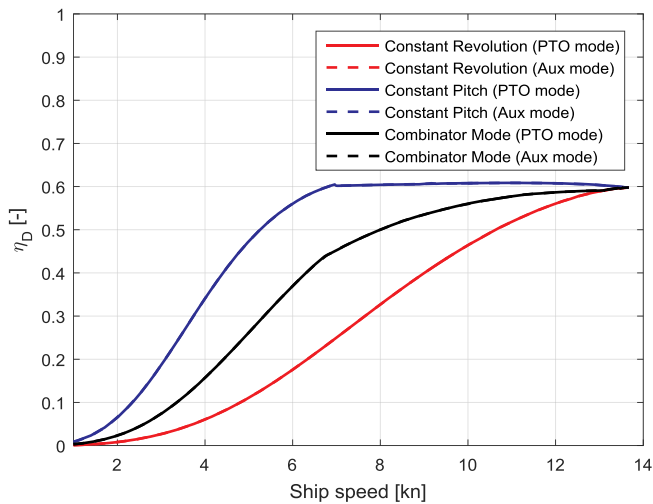


Fig. 13. Propulsive efficiency.

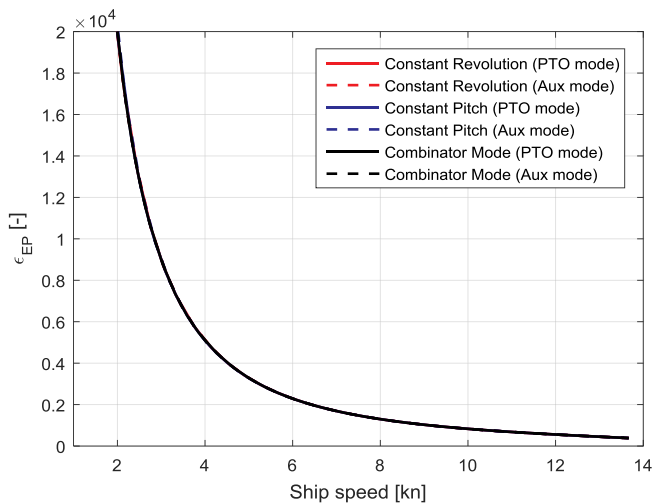


Fig. 14. Ship effective power effectiveness.

results in lower propulsive efficiency, so the propeller needs more power from engine for ship propulsion. The hub distribution factor ε_{hub} at PTO mode is slightly higher than that at Aux mode, because the engine power for electric system $P_{B,E}$ at PTO mode is slightly higher than that at Aux mode due to the power losses in the PTO gearbox. The transmission efficiency η_{TRM} of the shaftline does not change much with the ship speed and propulsion control modes, as shown in Fig. 12, having limited influence on the overall performance of the entire power chain.

The propulsive efficiency η_D shown in Fig. 13 is mainly determined by the propeller efficiency considering the fact that the ship hull efficiency does not vary too much under different operating conditions. At high ship speeds, the propulsive efficiency under different propulsion control modes shows very small differences because both the propeller speed and pitch are almost the same to obtain the corresponding high ship speeds. When the ship slows down, the propulsive efficiency under all the three different propulsion control modes decreases as a result of the different combinations of propeller speed and pitch to obtain the required low ship speeds. The decrease of propulsive efficiency under constant revolution propulsion control mode is the fastest, followed by the combinator control mode while for the constant pitch control mode the propulsive efficiency changes slowest as shown in Fig. 13. In other words, the constant pitch control mode shows the best propulsive efficiency when the ship sails at low speeds while the constant revolution mode has the worst propulsive efficiency and the combinator control

modes lies in between. When the ship is operating under constant revolution mode, in order to reduce the ship speed, the propeller pitch has to be reduced, consequently decreasing the propeller efficiency. In fact, the propeller pitch has a dominating effect on the propeller efficiency while the propeller speed hardly has an influence when the ship sails under certain resistance conditions.

The ship effective power effectiveness ε_{EP} , i.e. the ratio of ship dead weight to resistance W_D/R , under the three different propulsion control modes will be obviously the same when the ship sails at the same speeds, as shown in Fig. 14. When the ship slows down, the ship effective power effectiveness ε_{EP} will increase accordingly, in other words, the power needed for ship propulsion to transport a certain useful load will be reduced significantly when reducing the ship speed. As a consequence, the required engine power will be reduced by a great deal when the ship sails at low speeds especially when the propulsive efficiency η_D does not change much, for example when the ship is operated under the constant pitch control modes or the ship is propelled by a fixed pitch propeller that is the most common case for large ocean-going cargo ships nowadays. In fact, the ship effective power effectiveness ε_{EP} is the core reason why ship transportation is the most efficient when compared to other transportation modes and the absolute size of useful weight W_D makes it the most important transportation mode in terms of transport volume as well.

5.4.3. Summary of the results

The result of course is that slow steaming within a certain ship speed range will reduce the fuel consumption. Generating the electric power by the shaft generator (PTO mode) rather than by the auxiliary generators (Aux mode) also saves fuel. Constant revolution control mode consumes more fuel than the other two modes especially at low ship speeds. However, the benchmark chemical tanker operates in constant revolution mode most of the time during transport because of the installed shaft generator, which needs to run at constant revolution. When the ship is operating at constant pitch and combinator modes, where the shaft speed will change significantly with SLC, the onboard electric power will be provided by the auxiliary generators rather than the shaft generator to provide electricity with stable frequency and voltage for the onboard grid.

When comparing the fuel index and energy conversion effectiveness of the ship under constant revolution mode, where the electric power is generated in PTO mode, with those under constant pitch and combinator modes, where the electric power is generated in Aux mode, the disadvantages brought by the constant revolution mode at low ship speeds are essentially the results of the decreased propeller pitch, leading to a lower propeller efficiency which is not compensated by the better specific fuel consumption of the engine and the advantages of the shaft generator.

6. Conclusions and recommendations

This paper has cleared up some confusion in the existing terminology by developing a consistent and comprehensive theoretical framework of the energy conversion of ships. With the new framework, in addition to having an overall look at the whole power chain, this paper also has a close look inside the stages of the energy conversion process, providing a deeper insight into the influence of individual nodes and links of the power chain on the overall performance. The influence on the transport performance by ship operations is provided through a quantitative and systematic investigation on the impact of operational reduction of ship speeds, propulsion control modes and electric power generation modes.

According to results of the ship performance investigation, the most efficient and practical way to reduce the fuel index of a cargo ship not surprisingly is to reduce the ship speed. However, the engine specific fuel consumption may increase with the reduction of the ship speed, which is a misleading result. In this paper *operational* reduction of ship speed has been investigated given a fixed nominal or design speed. In fact, under IMO, ships are designed to be slower by selecting propulsion systems

with smaller engines in the design stage to achieve a lower EEDI, which has raised serious concerns regarding ship safety in adverse weather conditions. However, designing the ship for a higher speed but reducing *actual* operational speed during missions will be more effective and safer.

Alternative propulsion control modes also result in differences in the fuel consumption performance especially at low ship speeds. In terms of the fuel index, the constant pitch control mode shows the best performance during various operational conditions while the constant revolution model is the worst especially during low ship speeds. In terms of the specific fuel consumption of the engines, the constant revolution mode shows a better behaviour compared with the other two control modes in particular at low ship speeds. But this is a misleading result. The propulsive efficiency and the effective power effectiveness are the core factors that have a dominating influence on the overall performance of the power chain. The effective power effectiveness presents the core reason why bigger and slower ships are more efficient. However, the reduction of the propulsive efficiency at lower ship speed will severely limit the increase of the energy conversion effectiveness that would be possible from the effective power effectiveness, i.e. the favourable weight/resistance ratio at low speeds.

The energy management of the power chain, which is quantified by the hub distribution factor, has a large impact on the energy conversion effectiveness of the ship. The more the power is distributed for ship

propulsion compared to the power provided for example to the electrical loads onboard, the higher the energy conversion effectiveness will be, which means the ship will be more efficient. Investigation of the influence on the energy conversion effectiveness by the power-take-off (PTO) shows that, under the same propulsion control mode, generating the electric power by the shaft generator rather than the auxiliary generator also reduces fuel consumption of the ship but the effect is relatively minor.

Last but not least, there are still some uncertainties and limitations in this study and these need to be further studied in future work. The main uncertainties are present in the prediction of the fuel consumption performance of the 2-stroke diesel engine because of a small database as introduced in [Appendix B](#). It is the intention to try to obtain more test data through further cooperation with partners from industry. The main limitation is that in this paper only *point* values of the performance parameters are investigated while in the end *mean* values weighted over realistic mission profiles must give the real answers.

Acknowledgements

This project partly is financially supported by ‘International Science & Technology Cooperation Program of China’, 2014DFA71700; Marine Low-Speed Engine Project-Phase I.

Appendix A. Description of component models

A.1. Normalisation of Variables

For the sake of convenience in modelling and analysis of the ship propulsion system, some variables used in the model of ship propulsion system have been normalised by relating the off-design condition variables to the corresponding variables of a known nominal condition ([Klein Woud and Stapersma, 2002](#)) as presented in Eq. (A. 1).

$$X^* = \frac{X}{X_{nom}} \quad (\text{A1})$$

Where, X^* is the normalised variables, X is the relevant variables to be normalised and X_{nom} is the corresponding nominal value of the variables. Note that the mathematical technique of normalisation is the same as relating sea trial to prediction as was done to make corrections for the actual sea trial measurements.

A.2. Diesel engine model

In this paper, an analytical and first principle model in which the engine torque M_{eng} is modelled as a function of engine speed n_{eng} and the injected fuel per cycle m_f ([Shi, 2013](#)) expressed by Eq. (A2). has been adopted in the ship propulsion system model. The engine torque M_{eng} , injected fuel per cycle m_f and the engine speed n_{eng} have all been normalised as M^* , m_f^* and N^* according to Eq. (A. 1).

$$\begin{aligned} M^* &= f(m_f^*, N^*) \\ &= f_1(m_f^*) + f_2(N^*) + f_3(m_f^*, N^*) \\ &= 1 - a \cdot (1 - m_f^*) + b \cdot (1 - m_f^*)^2 - c \cdot (1 - N^*) + d \cdot (1 - N^*)^2 \\ &\quad + 2 \cdot e \cdot (1 - m_f^*) \cdot (1 - N^*) \end{aligned} \quad (\text{A2})$$

This equation essentially is a Taylor series approximation of a function of two variables up to second order terms, including the cross product.

A.3. Ship resistance model

Most of the time the ship resistance or ship effective power are modelled when modelling ship resistance characteristics, however, unfortunately this kind of models are not first principle because they just model the results rather than the physics behind the final results, in other words, one cannot have a physical insight in the modelled system. In ([Klein Woud and Stapersma, 2002](#)) the specific resistance of ship hull C_E , which is a non-dimensional parameter indicating the ship resistance characteristics when amongst others ship size, speed and hull form are given. It is defined by Eq. (A. 3).

$$C_E = \frac{P_E}{\rho \cdot \nabla^{2/3} \cdot v_s^3} \quad (\text{A3})$$

Where, P_E is the ship effective power (W); ρ is the density of water (kg/m^3); ∇ is the displacement volume of the hull (m^3); v_s is the ship velocity (m/s).

In this paper, the ship specific resistance C_E instead of ship resistance or ship effective power, which is the result of the former, is modelled as a

function of ship speed v_s by Eq. (A. 4). The variables in the following equations have been normalised according to Eq. (A. 1). Both the viscous resistance at lower ship speeds and wave-making resistance at higher ship speeds are modelled by Eq. (A. 4). The wave-making resistance, which takes a very small part of the total resistance at low ship speeds and will increase rapidly at high ship speeds, is modelled as an exponential function of the ship speed. The viscous resistance consists of the basic viscous resistance, a linear correction and nonlinear correction, the latter two contributions being the result of viscous effect at lower Reynolds and being modelled as a linear slope and exponential function respectively.

$$C_E^* = \underbrace{1 - a_{CE}}_{\text{Basic viscous resistance}} + \underbrace{k_{CE} \cdot (v_s^* - 1)}_{\text{Linear correction viscous resistance}} + \underbrace{c_{CE} \cdot (e^{d_{CE} \cdot v_s^*} - e^{d_{CE}})}_{\text{Nonlinear correction viscous resistance}} + \underbrace{a_{CE} \cdot e^{b_{CE} \cdot (v_s^* - 1)}}_{\text{Wavemaking resistance}} \quad (\text{A4})$$

Viscous Resistance

A.4. Propeller model

The propeller model introduced in (Klein Woud and Stapersma, 2002) has been applied in this paper, as shown in Eq. (A. 5) and Eq. (A. 6).

$$K_T^* = 1 + a_{prop} \cdot (J^* - 1) + c_{prop} \cdot (J^* - 1)^2 \quad (\text{A5})$$

$$K_Q^* = 1 + b_{prop} \cdot (J^* - 1) + d_{prop} \cdot (J^* - 1)^2 \quad (\text{A6})$$

The propeller thrust coefficient K_T , torque coefficient K_Q and advance ratio J have been normalised as K_T^* , K_Q^* and J^* according to Eq. (A. 1).

A.5. Wake factor, thrust deduction factor and relative rotative efficiency model

In this paper, the wake factor w , thrust deduction factor t and relative rotative efficiency η_R are modelled as a quadratic function of ship speed v_s by Eq. (A. 7), Eq. (A. 8) and Eq. (A. 9) respectively. The variables in the equations have already been normalised by Eq. (A. 1).

$$w^* = 1 - c_w \cdot (1 - v_s^*) + d_w \cdot (1 - v_s^*)^2 \quad (\text{A7})$$

$$t^* = 1 - c_t \cdot (1 - v_s^*) + d_t \cdot (1 - v_s^*)^2 \quad (\text{A8})$$

$$\eta_R^* = 1 - c_{\eta R} \cdot (1 - v_s^*) + d_{\eta R} \cdot (1 - v_s^*)^2 \quad (\text{A9})$$

Again, these essentially are Taylor series approximations of a function of one variable up to second order terms.

A.6. Mechanical transmission losses

The method proposed in (Godjevac et al., 2016) is used to model the transmission losses of propulsion shaftline and PTO gearbox of the ship. The gearbox and shaft losses are presented as a torque loss M_{loss} , which is expressed as function of the input torque M_{in} and input speed N_{in} , shown in Eq. (A. 10). The variables in the equation have already been normalised.

$$M_{loss}^* = k_a \cdot M_{in}^* + k_b \cdot N_{in}^* + k_c \quad (\text{A10})$$

Where, k_a is the coefficient related to the torque, k_b is the coefficient related to the rotational speed and k_c is the coefficient related to the constant torque loss.

Appendix B. Calibration of component models to testbed and towing tank measurements

B.1. Diesel Engine

The calibration results of diesel engine model are shown in Table B 2, Fig. B 1 and Fig. B 2. The engine test data used in calibrating the diesel engine torque model are selected from operating points along the propeller curve and the generator curve in the engine envelope. Fuel consumption test data of operating points along the generator curve and propeller curve are obtained by taking the mean value of the corresponding data of the EIAPP (Engine International Air Pollution Prevention) technical files of five different engines from the same engine family including the diesel engine installed in the chemical tanker as shown in Table B 1. The mean value of data of different engines is taken in the following way, firstly, the mean value of data of different engines at nominal points are taken as the new nominal value of the engine; secondly, the mean values of part load percentages, i.e. the ratios of part load value to nominal value, along generator curve (E2 cycle) and propeller curve (E3 cycle) of different engines are taken as the part load percentages of the engine along generator curve and propeller curve respectively.

Table B1

Available EIAPP test data of MAN6S35ME engines from the same engine family

Test cycle	E2	E3	E3	E3	E3
Rated Power (kW)	4170	5220	4500	4050	3320
Rated speed (rpm)	167	167	144	142	132

Table B2
Coefficients of engine torque model

Nominal Parameters			Coefficients				
$M_{eng,nom}$ [kNm]	$m_{f,nom}$ [g/cyl/cycle]	$n_{eng,nom}$ [rpm]	a	b	c	d	e
238.4465	12.2769	167	-0.0099	-0.2046	0.9342	-0.1056	0.0179

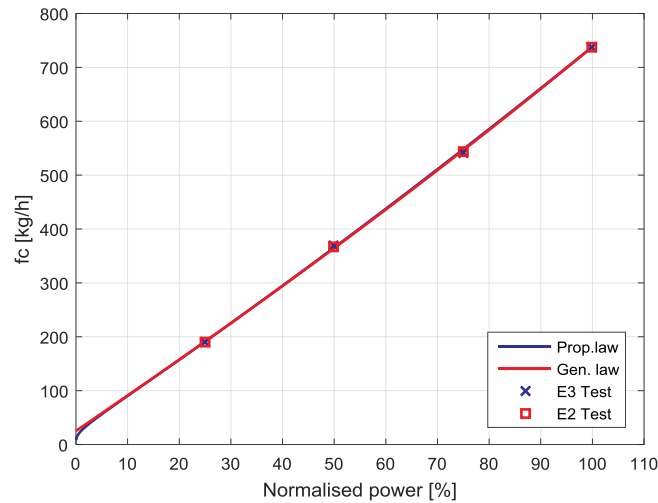


Fig. B1. Fuel Consumption Flow.

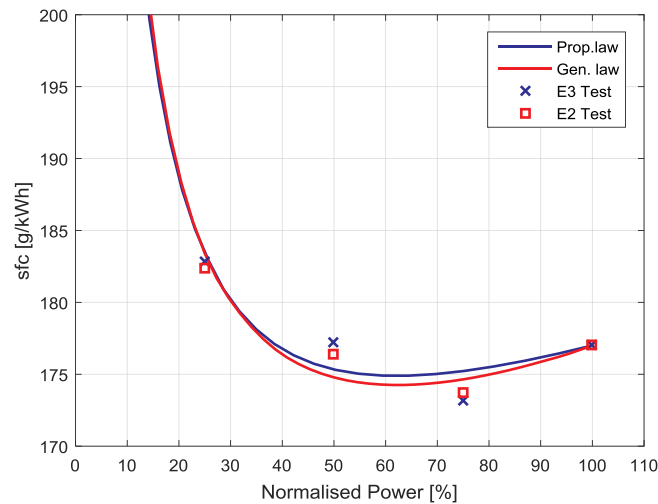


Fig. B2. Specific Fuel Consumption.

From the above model results it is found that the fuel consumption performance of a 2-stroke diesel engine is different from that of a 4-stroke diesel engine. The specific fuel consumption of 4-stroke diesel engines is better (lower) when the engine is operating under the propeller law than under the generator law (Klein Woud and Stapersma, 2002). However, the 2-stroke diesel engine investigated in this paper has better specific fuel consumption when operating under generator law than the propeller law, although in fact there is hardly any difference as shown in Fig. B 2, which is also different from 4-stroke diesel engine. Unfortunately, very few data in this regard are found in the open literature and currently we have limitations to prove the accuracy of our model results. More data and research results in this regard are expected and encouraged to be published by the other researchers.

B.2. Ship resistance

The calibration results of ship resistance model are shown in Table 4 and B3, Fig. B 3 and Fig. B 4. Note that the original model test data of ship effective power presented in Fig. B 4 have been corrected together with the original model test data of the propeller open water characteristics according to the real ship sea trial test results and the correction method as was shown in the main text (section 4.2). In addition, the available test data are limited in the high ship speeds range, namely from 11.5kn to 15kn, and there is no data available for the low ship speeds below 11.5kn. Therefore, only the specific ship resistance model at high ship speeds are calibrated using the available test data while the model at low ship speeds are fitted according to the ship resistance calculation method presented in (Holtrop and Mennen, 1982; Holtrop, 1984) carried out by the authors but not presented here.

Table B3
Coefficients of Ship Resistance Model

Nominal Parameters		Coefficients				
$1000C_{E,nom}$ [-]	$v_{s,nom}$ [kn]	a_{CE}	b_{CE}	c_{CE}	d_{CE}	k_{CE}
10.6863	15	0.333	10.2	0.07	-15	-0.06

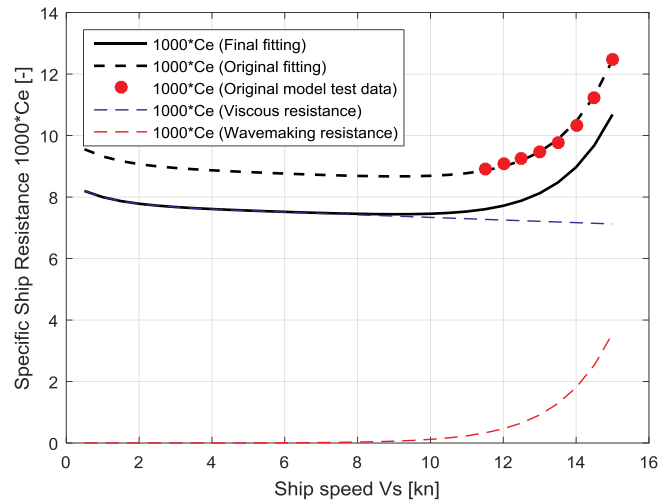


Fig. B3. Specific Ship Resistance.

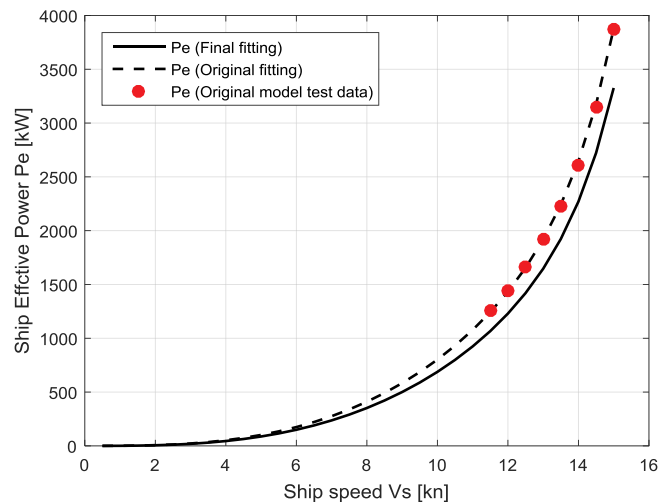


Fig. B4. Ship Effective Power.

B.3. Propeller

The calibration results of propeller model are shown in [Table B4](#) and [Fig. B 5](#). Note that as mentioned before, the original model test data of the propeller open water characteristics have been corrected together with the original model test data of the ship effective power according to the ship sea trial test results as show in the main text (section 4.2).

Table B4
Coefficients of Propeller Model

Nominal Parameters			Coefficients			
$K_{T,nom}$ [-]	$10K_{Q,nom}$ [-]	J_{nom} [-]	a_{prop}	b_{prop}	c_{prop}	d_{prop}
0.1597	0.1942	0.4072	-1.0551	-0.8018	-0.1227	-0.1346

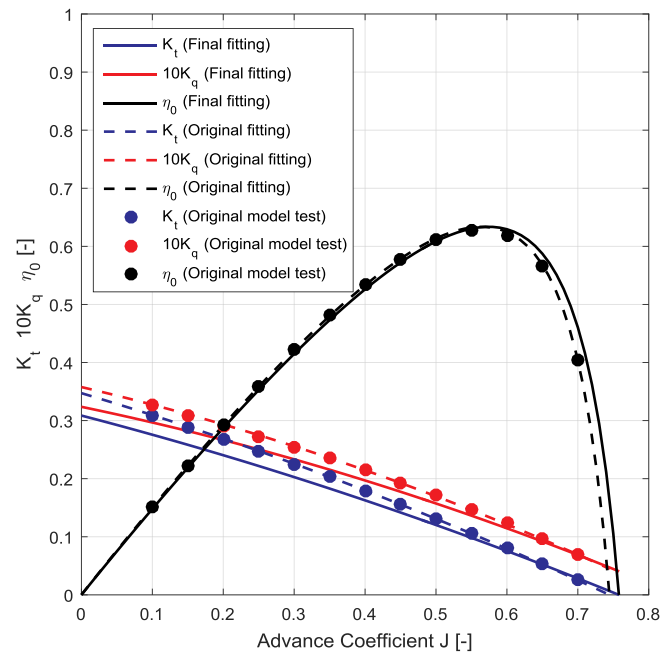


Fig. B5. Propeller Open Water Characteristics.

B.4. Wake factor, thrust deduction factor and relative rotative efficiency

The calibration results of models of wake factor, thrust deduction factor and relative rotative efficiency are shown in Table B 5, Fig. B 6 and Fig. B 7. Note that the model test data of the wake factor, thrust deduction factor and relative rotative efficiency remains the same as the original model test data while the delivered power, propeller speed, ship effective power and propeller characteristics of the original model test data have been corrected according to the real ship sea trial test data as shown in the main text (section 4.2).

Table B5

Coefficients of wake factor, thrust deduction factor and relative rotative efficiency models

(a) Coefficients of wake factor model			
Nominal Parameters		Coefficients	
w_{nom} [-]	$v_{s,nom}$ [kn]	c_w	d_w
0.2781	12.5	0.0880	0.1059
(b) Coefficients of thrust deduction factor model			
Nominal Parameters		Coefficients	
t_{nom} [-]	$v_{s,nom}$ [kn]	c_t	d_t
0.2009	12.5	0.0110	0.0147
(c) Coefficients of relative rotative efficiency model			
Nominal Parameters		Coefficients	
$\eta_{R,nom}$ [-]	$v_{s,nom}$ [kn]	$c_{\eta r}$	$d_{\eta r}$
0.9808	12.5	0.0235	0.0279

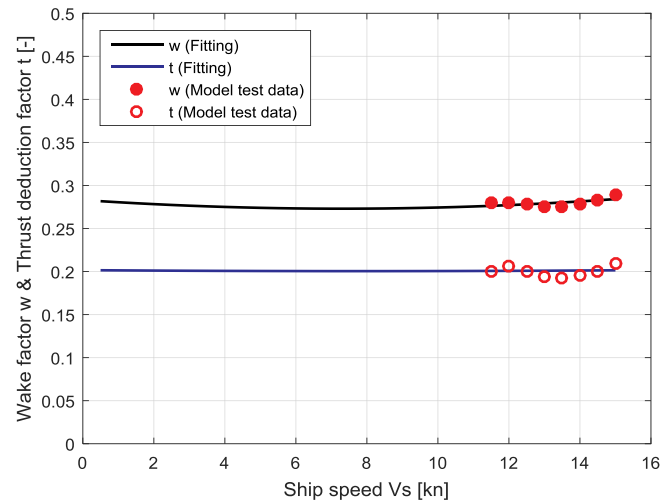


Fig. B6. Wake factor and Thrust deduction factor.

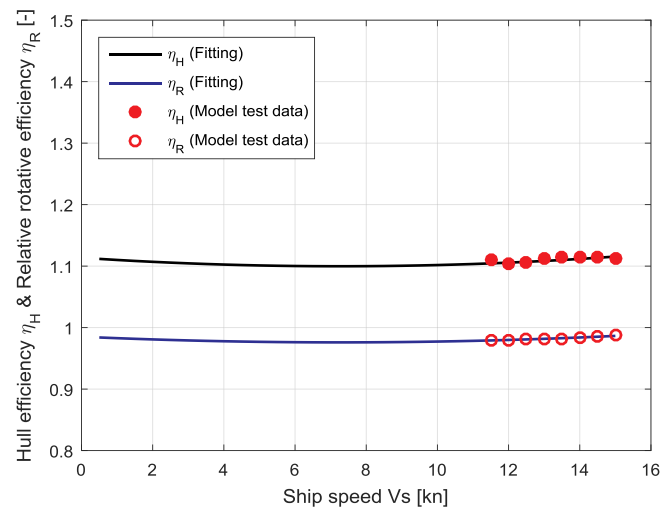


Fig. B7. Hull efficiency and Relative rotative efficiency.

References

- Akagi, S., 1991. Synthetic aspects of transport economy and transport vehicle performance with reference to high speed marine vehicles. In: Proceeding 1st International Conference on Fast Sea Transportation - FAST, vol. 91 (Trondheim).
- Akagi, S., Morishita, M., 2001. Transport economy-based evaluation and assessment of the use of fast ships in passenger-car ferry and freighter systems. In: Proceeding 6th International Conference on Fast Sea Transportation - FAST 2001 (London).
- Altosole, M., Borlenghi, M., Capasso, M., Figari, M., 2007. Computer-based design tool for a fuel efficient-low emissions marine propulsion plant. Proceedings of the 2nd International Conference on Marine Research and Transportation (ICMRT 2007), Ischia, Naples, Italy.
- Andersson, K., Baldi, F., Brynolf, S., Lindgren, J.F., Granhag, L., Svensson, E., 2016. Shipping and the Environment.
- Armstrong, V.N., Banks, C., 2015. Integrated approach to vessel energy efficiency. *Ocean. Eng.* 110, 39–48.
- Asprion, J., Chinellato, O., Guzzella, L., 2013. A fast and accurate physics-based model for the NOx emissions of Diesel engines. *Appl. Energy* 103, 221–233.
- Bialystocki, N., Konovessis, D., 2016. On the estimation of ship's fuel consumption and speed curve: a statistical approach. *J. Ocean. Eng. Sci.* 1 (2), 157–166.
- Bitner-Gregerse, E.M., Soares, C.G., Vantorre, M., 2016. Adverse Weather Conditions for Ship Manoeuvrability, 14, 1631–1640.
- Bossel, H., 1994. Modeling and Simulation. A K Peters/CRC Press, New York.
- Buhaug, Ø., Corbett, J.J., Endresen, Ø., Eyring, V., Faber, J., Hanayama, S., Lee, D.S., Lee, D., Lindstad, H., Markowska, A.Z., 2009. Second Imo Ghg Study 2009. International Maritime Organization (IMO), London, UK, p. 20.
- Coraddu, A., Figari, M., Savio, S., 2014. Numerical investigation on ship energy efficiency by Monte Carlo simulation. *Proc. Inst. Mech. Eng. M J. Eng. Marit. Environ.* 228 (3), 220–234.
- Coraddu, A., Oneto, L., Baldi, F., Anguita, D., 2015. Ship Efficiency Forecast Based on Sensors Data Collection: Improving Numerical Models through Data Analytics. *OCEANS 2015. IEEE.*, Genova, pp. 1–10.
- Del Re, L., Allgöwer, F., Glielmo, L., Guardiola, C., Kolmanovsky, I., 2010. Automotive Model Predictive Control: Models, Methods and Applications. Springer, Berlin.
- Eyring, V., Isaksen, I.S.A., Berntsen, T., Collins, W.J., Corbett, J.J., Endresen, O., Grainger, R.G., Moldanova, J., Schlager, H., Stevenson, D.S., 2010. Transport impacts on atmosphere and climate: Shipping. *Atmos. Environ.* 44 (37), 4735–4771.
- Faltinsen, O.M., 1980. Prediction of resistance and propulsion of a ship in a seaway. In: Proceedings of the 13th Symposium on Naval Hydrodynamics (Tokyo).
- Figari, M., Campora, U., 2003. Numerical simulation of ship propulsion transients and full-scale validation. *Proc. Inst. Mech. Eng. M J. Eng. Marit. Environ.* 217 (1), 41–52.
- Figari, M., Guedes Soares, C., 2009. Fuel consumption and exhaust emissions reduction by dynamic propeller pitch control. In: Guedes Soares, C., Das, P.K. (Eds.), *Analysis and Design of Marine Structures*, pp. 543–550.
- Gabrielli, G., Von Karman, T., 1950. What price speed? Specific power required for propulsion of vehicles. *Mech. Eng.* 72, 775–781.
- Geertsma, R.D., Negenborn, R.R., Visser, K., Hopman, J.J., 2017. Design and control of hybrid power and propulsion systems for smart ships: a review of developments. *Appl. Energy* 194, 30–54.
- Geertsma, R.D., Negenborn, R.R., Visser, K., Loonstijn, M.A., Hopman, J.J., 2017. Pitch control for ships with diesel mechanical and hybrid propulsion: modelling, validation and performance quantification. *Appl. Energy* 206, 1609–1631.
- Geertsma, R.D., Visser, K., Negenborn, R.R., 2018. Adaptive pitch control for ships with diesel mechanical and hybrid propulsion. *Appl. Energy* 228, 2490–2509.
- Godjevac, M., Drijver, J., de Vries, L., Stapersma, D., 2016. Evaluation of losses in maritime gearboxes. *Proc. Inst. Mech. Eng. M J. Eng. Marit. Environ.* 230 (4), 623–638.
- Grimmelius, H., Mesbahi, E., Schulten, P., Stapersma, D., 2007. The Use of Diesel Engine Simulation Models in Ship Propulsion Plant Design and Operation. CIMAC Congress.

- Guzzella, L., Onder, C., 2009. Introduction to Modeling and Control of Internal Combustion Engine Systems. Springer, Berlin.
- Harvald, S.A., 1983. Resistance and Propulsion of Ships. Wiley, New York.
- Holtrop, J., 1984. A statistical re-analysis of resistance and propulsion data. *Int. Shipbuild. Prog.* 31 (363), 272–276.
- Holtrop, J., Mennen, G.G., 1982. An approximate power prediction method. *Int. Shipbuild. Prog.* 29 (335), 166–170.
- Kanellos, F.D., Prousalidis, J.M., Tsekouras, G.J., 2014. Control system for fuel consumption minimization-gas emission limitation of full electric propulsion ship power systems. *Proc. Inst. Mech. Eng. M J. Eng. Marit. Environ.* 228 (1), 17–28.
- Kennell, C., 1998. Design trends in high-speed transport. *Mar. Technol. Sname News* 35 (3), 127.
- Klein Woud, H., Stapersma, D., 2002. Design of Propulsion and Electric Power Generation Systems. IMarEST, Institute of Marine Engineering, Science and Technology, London.
- Lee, C., Lee, H.L., Zhang, J., 2015. The impact of slow ocean steaming on delivery reliability and fuel consumption. *Transp. Res. E Logist. Transp. Rev.* 76 (Suppl. C), 176–190.
- Lindstad, H., Asbjørnslett, B.E., Jullumstrø, E., 2013. Assessment of profit, cost and emissions by varying speed as a function of sea conditions and freight market. *Transp. Res. D Transp. Environ.* 19 (Suppl. C), 5–12.
- Lindstad, H., Eskeland, G.S., 2015. Low carbon maritime transport: how speed, size and slenderness amounts to substantial capital energy substitution. *Transp. Res. D Transp. Environ.* 41 (Suppl. C), 244–256.
- MEPC, 2014. 2014 Guidelines on the method of calculation of the attained energy efficiency design index (EEDI) for new ships. Resolution MEPC 245, 66.
- Misra, S.C., 2016. Design Principles of Ships and Marine Structures. CRC Press, Boca Raton.
- Molland, A.F., Turnock, S.R., Hudson, D.A., 2011. Ship Resistance and propulsion Practical Estimation of Ship Propulsive Power. Cambridge university press, New York.
- Øyvind, E., Sørgeard, E., Sundet, J.K., Dalsøren, S.B., Isaksen, I.S.A., Berglen, T.F., Gravir, G., 2003. Emission from international sea transportation and environmental impact. *J. Geophys. Res. Atmos.* 108 (D17).
- Papanikolaou, A., 2005. Review of advanced marine vehicles concepts. In: Proceedings of the Seventh International Symposium on High Speed Marine Vehicles (HSMV 2005), pp. 21–23 (Naples, Italy).
- Papanikolaou, A., 2014. Ship Design: Methodologies of Preliminary Design. Springer, London.
- Papanikolaou, A., Zaraphonitis, G., Bitner-Gregersen, E., Shigunov, V., Moctar, O.E., Soares, C.G., Reddy, D.N., Sprenger, F., 2016. Energy efficient safe SHIP operation (SHOPERA). *Transp. Res. Procedia* 14, 820–829.
- Psarafitis, H.N., Kontovas, C.A., 2010. Balancing the economic and environmental performance of maritime transportation. *Transp. Res. D Transp. Environ.* 15 (8), 458–462.
- Psarafitis, H.N., Kontovas, C.A., 2013. Speed models for energy-efficient maritime transportation: a taxonomy and survey. *Transp. Res. C Emerg. Technol.* 26 (Suppl. C), 331–351.
- Refsgaard, J.C., Henriksen, H.J., 2004. Modelling guidelines—terminology and guiding principles. *Adv. Water Resour.* 27 (1), 71–82.
- Roskilly, A.P., Palacin, R., Yan, J., 2015. Novel technologies and strategies for clean transport systems. *Appl. Energy* 157 (Suppl. C), 563–566.
- Schulten, P.J.M., 2005. The Interaction between Diesel Engines, Ship and Propellers during Manoeuvring.
- Shi, W., 2013. Dynamics of Energy System Behaviour and Emissions of Trailing Suction Hopper Dredgers.
- Stapersma, D., 2010. Diesel Engines - A Fundamental Approach to Performance Analysis, Turbocharging, Combustion, Emissions and Heat Transfer. Emissions and Heat Transfer, Part II: Diesel Engines B - Combustion, Emissions and Heat Transfer. Lecture Notes NLDA/TU Delft April 2010. NLDA & Delft UT, Delft.
- Stapersma, D., 2016. Some thoughts on an energy efficiency design index for naval ships. In: 13th International Naval Engineering Conference. INEC 2016), Bristol UK.
- Stapersma, D., 2017. Main Propulsion Arrangement and Power Generation Concepts. John Wiley & Sons, Ltd.
- Sui, C., Song, E., Stapersma, D., Ding, Y., 2017. Mean value modelling of diesel engine combustion based on parameterized finite stage cylinder process. *Ocean. Eng.* 136, 218–232.
- UNCTAD, 2017. Review of Maritime Transport 2017. UNITED NATIONS PUBLICATION, New York and Geneva.
- Vrijdag, A., 2009. Control of Propeller Cavitation in Operational Conditions.
- Yasukawa, H., Zaky, M., Yonemasu, I., Miyake, R., 2017. Effect of Engine Output on Maneuverability of a VLCC in Still Water and Adverse Weather Conditions, pp. 1–13.